Supplementary information for:

Terminal hydride formation in [FeFe] hydrogenase: understanding the role of the dithiolate bridgehead

Anjali Depala[a], Manon T. Lachmann[b], Simone Morra[c], James A. Birrell*[d] and Patricia Rodríguez-Maciá*[b]

[a]Department of Chemistry, University of Oxford, Inorganic Chemistry laboratory, South Parks Road, Oxford, OX1 3QR, UK

[b]School of Chemistry and Leicester Institute for Structural and Chemical Biology, University of Leicester, University Road, Leicester, LE1 7RH, UK

[c]University of Nottingham, Faculty of Engineering, Coates Building, University Park, Nottingham, NG7 2RD

[d]School of Life Sciences, University of Essex, Wivenhoe Park, Colchester, CO4 3SQ, UK

Table of contents:

Materials and Methods

Sample preparation

*Cr*HydA1 apoenzyme (containing the $[4Fe\text{-}4S]_H$ cluster but lacking $[2Fe]_H$) was produced and maturated with $(Et_4N)_2[Fe_2(pdt)(CO)_4(CN)_2]$ as previously described.[1, 2 3]

Infrared (IR) spectroscopy

IR samples were prepared in an anaerobic glovebox (Glove Box Technology Ltd. UK) under an N_2 atmosphere by mixing 4 µL of enzyme in 20 mM Tris, 30 mM NaCl buffer pH 8 with either reductant or oxidant before sandwiching the sample between two CaF_2 windows (Crystan) with a 50 µm Teflon spacer (PIKE technologies), and sealing them inside a commercial IR cell (PIKE technologies). Inside an anaerobic glovebox (Glove Box Technology Ltd. UK), IR spectra were collected using a Bruker VERTEX 80 FTIR spectrometer equipped with a mercury cadmium telluride (MCT) detector that was cooled with liquid nitrogen. Spectra were recorded using OPUS software with a resolution of 2 cm^{-1}, aperture setting of 1 mm, and a scan velocity of 20 kHz with an average of 1024 scans. Once recorded, water vapour subtraction and data cutting were completed in OPUS, followed by baseline subtraction as described later. Sodium dithionite and hexaammineruthenium(III) chloride were added to 10 mM from 100 mM stocks in 100 mM Tris, 150 mM NaCl buffer pH 8. Eu(II)-diethylenetriamine pentaacetate (DTPA) was prepared by first dissolving $EuCl_2$ in 0.5 M HCl to a concentration of 100 mM and diethylenetriamine pentaacetic acid in 0.5 M NaOH to 100 mM. The two solutions were then mixed in a 1:1 ratio to produce a 50 mM Eu(II)-DTPA solution. pH indicator paper was used to ensure the pH was close to neutral, and the solution was slowly added to the enzyme to a final concentration of 10 mM Eu(II)-DTPA (unless otherwise stated).

Electron paramagnetic resonance (EPR) spectroscopy

EPR samples were prepared in an anaerobic glovebox (Coy) under an atmosphere of 2% H_2/98% N_2 by mixing 160 µL of 0.25 mM enzyme in 100 mM Tris-HCl, 150 mM NaCl buffer pH 8 with 40 µL 50 mM Eu(II)-DTPA. Samples were frozen in liquid nitrogen and measured at 20 K and 10 µW power on a Bruker E500 X-band (9.36 GHz) EPR spectrometer. Sample temperature was maintained with liquid helium using an Oxford Instruments transfer line and an ITC temperature controller. EPR spectra were collected with 100 kHz modulation frequency, 10 Gauss modulation amplitude, and 80 ms time constant. IR and EPR spectra were analysed, and background subtracted using Kazan Viewer in the MATLAB environment, and EPR spectral simulations were performed using the esfit function in EasySpin also in MATLAB.

Supplementary Figures

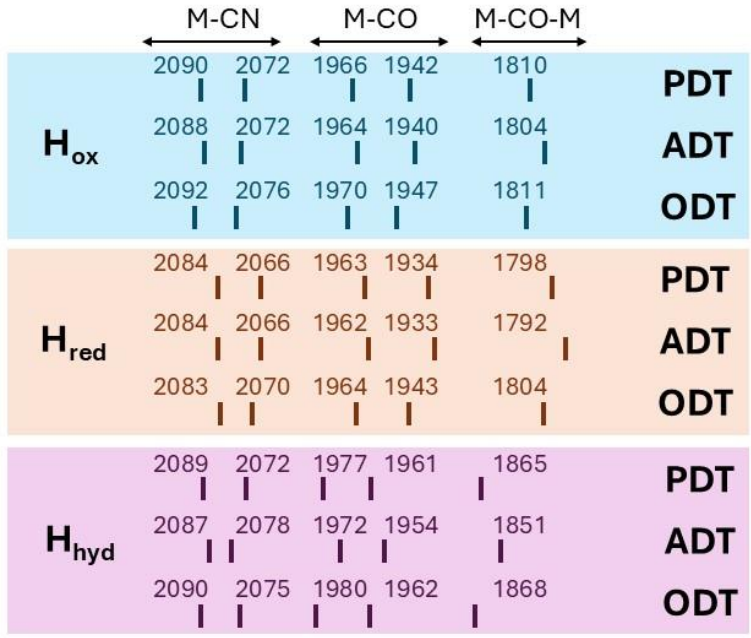

Figure S1 – IR vibrational frequencies of *Cr*HydA1 maturated with the PDT, ADT or ODT cofactors poised in the H_{ox}, H_{red} and H_{hyd} redox states. All IR frequencies for Hox and Hred are taken from Table S1 in Duan *et al.*[4] IR frequencies for ODT H_{hyd} are from Reijerse *et al.*[5] IR frequencies for H_{hyd} are for $H_{hyd:red}$ and are taken from Lorent *et al.*[6] IR frequencies for PDT H_{hyd} are from this work.

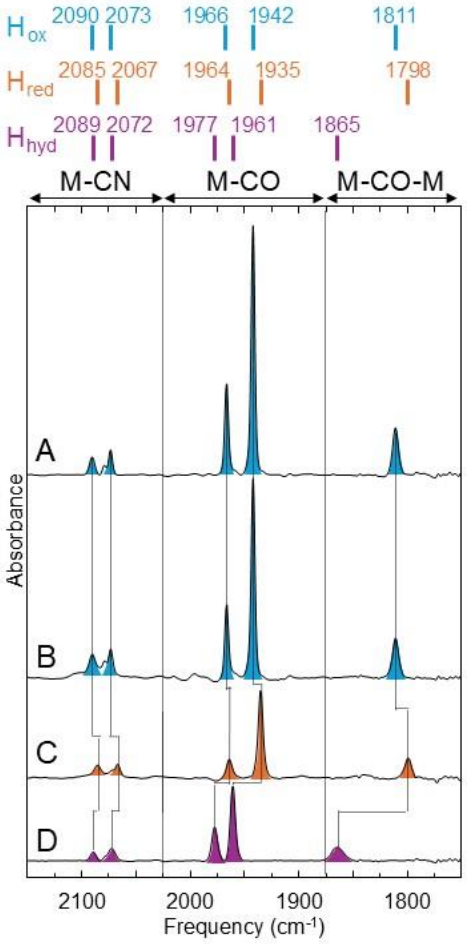

Figure S2 – IR spectra of 1.3 mM *Cr*HydA1^{PDT} as isolated (A), oxidised with 10 mM hexaammineruthenium (III) chloride (B), reduced with 10 mM sodium dithionite (C) and reduced with Eu(II)-DTPA (D). The IR bands assigned to the H_{ox}, H_{red} and H_{hyd} states are coloured blue, orange and purple, respectively.

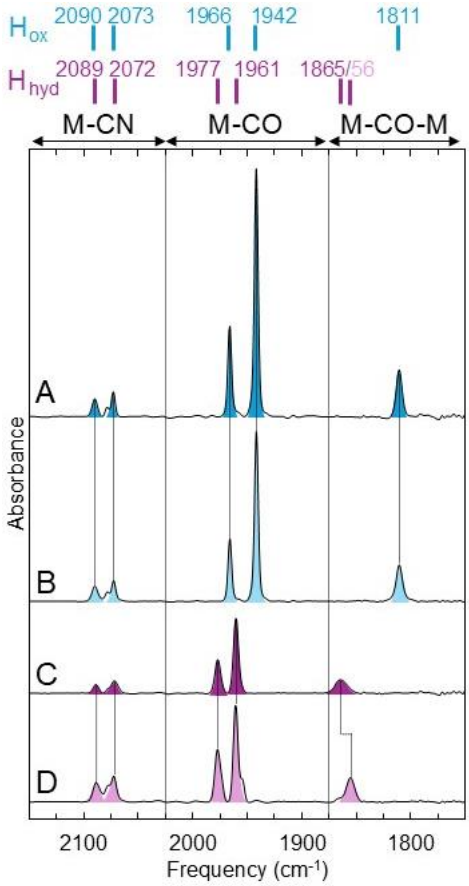

Figure S3 – IR spectra of 2.3 mM *Cr*HydA1^{PDT} as isolated (A, B) and reduced with 10 mM Eu(II)-DTPA (C, D). A and C were measured in H_2O, while B and D were measured in D_2O. The IR bands assigned to the H_{ox} and H_{hyd} states are coloured blue and purple, respectively.

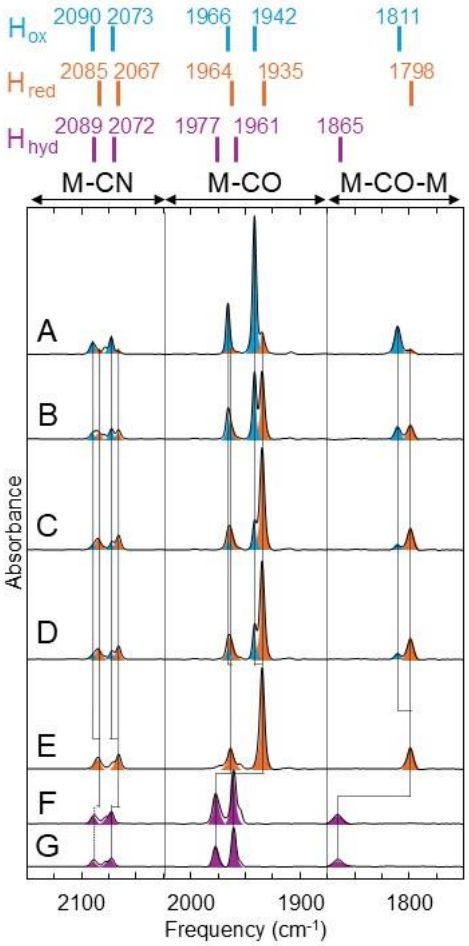

Figure S4 – FTIR spectra of 3.2 mM *Cr*HydA1^{PDT} samples with increasing concentrations of Eu(II)-DTPA: A) 0 mM, B) 1 mM, C) 2 mM, D) 4 mM, E) 6 mM, F) 8 mM, G) 10 mM. The IR bands assigned to the H_{ox}, H_{red} and H_{hyd} states are coloured blue, orange and purple, respectively.

A)

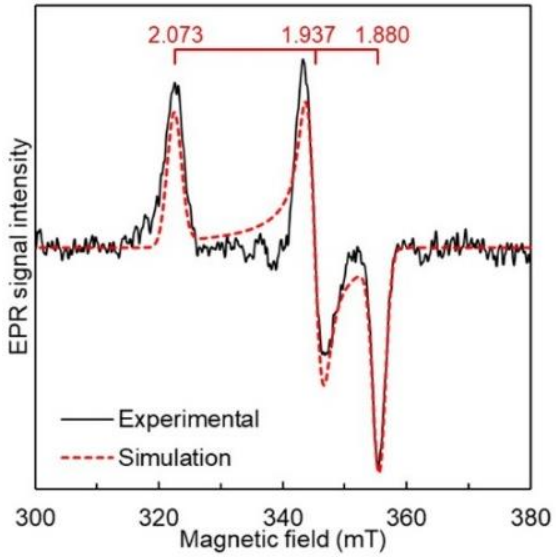

B)

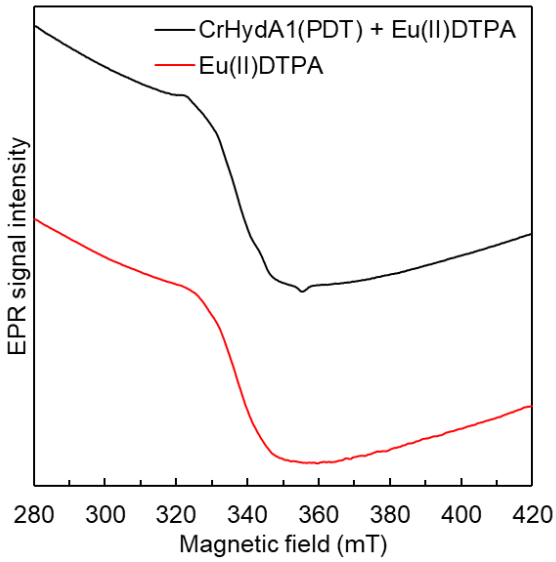

Figure S5 – A) EPR spectrum of *Cr*HydA1^{PDT} reduced with Eu(II)-DTPA. The spectrum was generated by subtracting the broad Eu(II)-DTPA component. Simulation was performed in Easyspin, yielding a rhombic EPR spectrum with g-values of 2.073, 1.937 and 1.880. B) Raw EPR spectra of 200 µM *Cr*HydA1^{PDT} reduced with 10 mM Eu(II)-DTPA (black trace) and 10 mM Eu(II)-DTPA alone (red trace). The spectra were measured at X-band (9.36 GHz), 20 K and 10 µW power. All other experimental details are reported in the Materials and Methods.

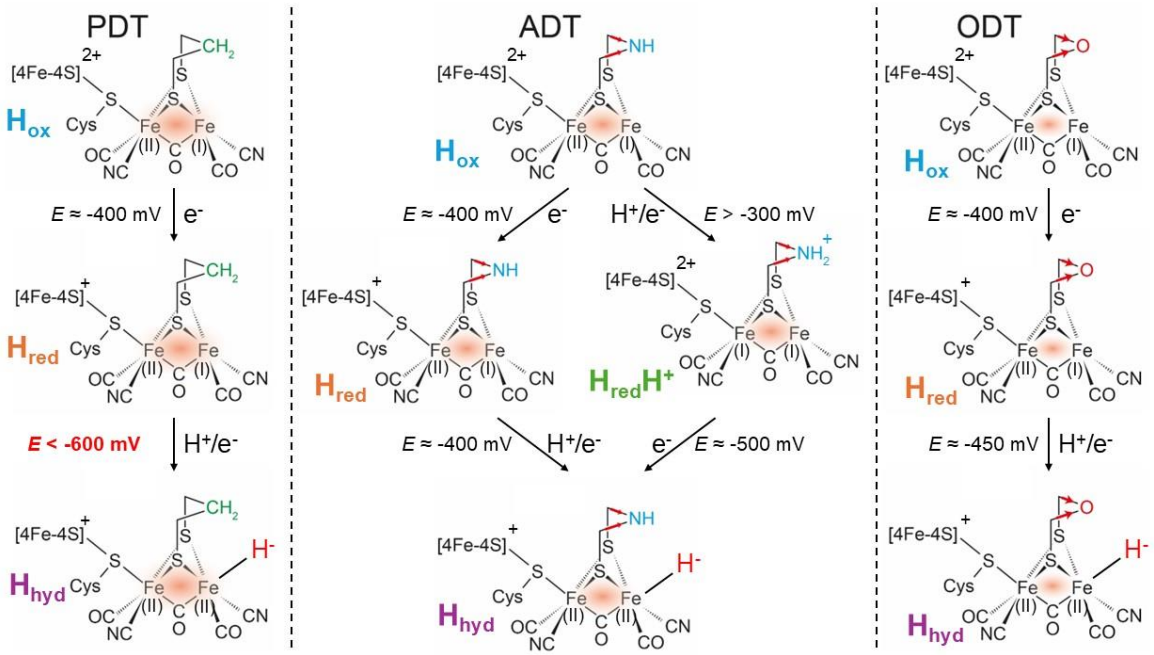

Figure S6 Proposed pathways of H_{hyd} generation in [FeFe] hydrogenases containing the PDT, ADT and ODT ligands. The native, ADT-containing enzyme in H_{ox} is doubly reduced (on $[4Fe\text{-}4S]_H$ and $[2Fe]_H$) and protonated at the ADT bridgehead yielding $H_{sred}H^+$ via either H_{red} or $H_{red}H^+$ intermediates. $H_{sred}H^+$ can tautomerise to H_{hyd}. Both reduction steps happen with redox potentials close to -400 mV. For both PDT and ODT, reduction of $[4Fe\text{-}4S]_H$ happens close to -400 mV (as the dithiolate ligand has only a minor influence on the $[4Fe\text{-}4S]_H$ redox potential). Reduction of $[2Fe]_H$ in both the PDT and ODT cases must proceed without protonation of the dithiolate bridgehead (cannot form $H_{sred}H^+$), and the redox potential will depend on the stability of H_{hyd}. Electron withdrawal from the bridgehead group (O in ODT and CH_2 in PDT) is predicted to influence the electron density on the Fe ions with O more electron withdrawing than C. Hence, reduction of $[2Fe]_H$ and H_{hyd} formation occurs at less negative potentials in the ODT enzyme than in the PDT enzyme.

Supplementary References

1. G. Berggren, A. Adamska, C. Lambertz, T. R. Simmons, J. Esselborn, M. Atta, S. Gambarelli, J. M. Mouesca, E. Reijerse, W. Lubitz, T. Happe, V. Artero and M. Fontecave, *Nature*, 2013, **499**, 66-69.
2. J. M. Kuchenreuther, C. S. Grady-Smith, A. S. Bingham, S. J. George, S. P. Cramer and J. R. Swartz, *PLOS ONE*, 2010, **5**, e15491.
3. J. Esselborn, C. Lambertz, A. Adamska-Venkatesh, T. Simmons, G. Berggren, J. Noth, J. Siebel, A. Hemschemeier, V. Artero, E. Reijerse, M. Fontecave, W. Lubitz and T. Happe, *Nature Chemical Biology*, 2013, **9**, 607-609.
4. J. Duan, S. Mebs, K. Laun, F. Wittkamp, J. Heberle, T. Happe, E. Hofmann, U.-P. Apfel, M. Winkler, M. Senger, M. Haumann and S. T. Stripp, *ACS Catalysis*, 2019, **9**, 9140-9149.
5. E. J. Reijerse, C. C. Pham, V. Pelmenschikov, R. Gilbert-Wilson, A. Adamska-Venkatesh, J. F. Siebel, L. B. Gee, Y. Yoda, K. Tamasaku, W. Lubitz, T. B. Rauchfuss and S. P. Cramer, *Journal of the American Chemical Society*, 2017, **139**, 4306-4309.
6. C. Lorent, S. Katz, J. Duan, C. J. Kulka, G. Caserta, C. Teutloff, S. Yadav, U.-P. Apfel, M. Winkler, T. Happe, M. Horch and I. Zebger, *Journal of the American Chemical Society*, 2020, **142**, 5493-5497.